Evidence of an Elastic Instability between the Amorphous and the Microcrystalline State of Ca-modified Lead Titanate as revealed by Brillouin Spectroscopy

J. K. Krüger,[1] C. Ziebert,[1] H. Schmitt,[1] B. Jiménez,[2] and C. Bruch[1]
[1]*Universität des Saarlandes, Fachbereich Physik, Bau 38, D-66123 Saarbrücken, Germany*
[2]*Instituto de Ciencia de Materiales de Madrid, Consejo Superior de Investigaciones Cientificas, Campus de Cantoblanco s/n, E-28049 Madrid, Spain*
(Received 28 October 1996)

Brillouin spectroscopy was used to probe the hypersonic properties of Ca-modified lead titanate between the pure amorphous and the coarse grained state. The samples were thin films rf sputtered onto (100)-silicon wafer at ambient temperature, followed by an annealing process in the range from 673 to 873 K. An elastic instability of the longitudinally polarized sound mode suggests the existence of a discontinuous structural transformation from the amorphous to the nanostructured state. [S0031-9007(97)02610-0]

PACS numbers: 81.05.Ys, 68.35.Rh, 68.60.Bs, 78.35.+c

Against the background of an increasing interest in nanostructured materials (nsM) the physical properties of the intermediate metastable structures between the pure amorphous and the microcrystalline states require special attention. One possible way to realize such intermediate states is to produce sputtered amorphous (dielectric) films and to anneal these films successively in an appropriate way. It is likely that the annealing-induced transformation from the initial amorphous state to the final coarse grained state may pass through one or more so-called metastable nanocrystallized states (e.g. [1–5]). It is a matter of current physical interest (i) whether these intermediate nanostructured states (nsS) can be fixed, (ii) how the transformation from the amorphous to the microcrystalline states takes place, and (iii) what are the properties of these intermediate states. Although the amorphous state as well as the nsS are metastable, the possibility of a structural phase transformation between the crystalline and the amorphous states has been proposed in the literature [1,5]. Based on free-energy simulations, Wang *et al.* [6], only recently, have predicted a phase transition from the nanocrystalline to the glassy state. A hint for the existence of such a transition may be drawn from the work of Rehn *et al.* [1]. These authors have reported an elastic shear instability for ion damaged Zr_3Al.

It is well established now that the evolution of the nsS is accompanied by an anomalous behavior in the elastic properties when compared to the amorphous and the microcrystalline reference states [2,4,7,8]. Experimental and theoretical results indicate a significant influence in the size of nanoparticles on the elastic properties of the consolidated nsM (e.g., [2,4,9–13]). In turn, the elastic properties are expected to reflect the predicted transition from the amorphous to the nsS. The aim of the current paper is to show evidences for such a transformation in rf-sputtered films of Ca-modified lead-titanate $(Pb_{0.76}Ca_{0.24})TiO_3$ (PTC) at a critical annealing temperature ($T_{ca} \approx 823$ K). As a sensitive probe we used the longitudinally polarized acoustic phonon mode as detected by high resolution Brillouin spectroscopy (BS).

PTC is—in the single or coarse grained polycrystalline state—a ferroelectric perovskite with a phase transition from the paraelectric to the ferroelectric state at $T_c \approx 530$ K [14]. At room temperature, the material is tetragonal with the point group 4MM. The lattice constants are $a = 0.3887$ nm and $c = 0.4091$ nm [15]. The mass density ρ, calculated from the x-ray data, is 7050 kg/m^3. In the present case, the samples were thin PTC films rf sputtered onto (100)-silicon substrates coated with a thin Ti layer as an adhesion promoter and diffusion barrier and a thin Pt layer as a bottom electrode. The as-sputtered films were amorphous. As measured by SEM, the samples were 1.2 μm thick, looked smooth, and showed no macroscopic pores. The exact Pb/Ti/Ca ratios of all samples were checked by energy-dispersive x-ray (EDX) analysis [16].

Table I gives the annealing temperatures T_a of the samples, the related grain size diameters d as determined by x-ray diffraction [16], and the Brillouin shifts f measured by backscattering. The annealing time was usually 30 min, and the samples were subsequently quenched to ambient temperature. As a reference, a coarse grained

TABLE I. Annealing temperatures T_a, related grain sizes d, and longitudinal acoustic phonon frequencies f.

Sample number	Annealing temperature T_a (K)	Grain size d (nm)	Brillouin shift f (GHz)
1	300	—	33.0
2	673	~1	30.7
3	773	~1	28.1
4	$T_{ca} \sim 823$	~35	32.2
			44.2
5	873	~46	42.3
6	1323	>1000	41.0

 0031-9007/97/78(11)/2240(4)$10.00

ceramic sintered at 1323 K was used. In none of the samples was a parasitic pyrochlore structure detected. While the evaluation of the main PTC-diffraction peaks of sample (4) led to a grain size of $d = 35$ nm, there was also a structured background indicating the coexistence of a second phase consisting of grains with much smaller size (subnanometer scale). It appeared that PTC in the nsS shows no tetragonal distortion and is therefore assumed to be cubic. The refractive index n was measured by ellipsometry. Within the margin of error n did not vary with T_a giving $n = 2.45 \pm 0.01$.

The BS measurements were performed at a laser wavelength of $\lambda_0 = 514.5$ nm using the 90A- and the 180-scattering geometries, respectively [17] (see insets in Figs. 1 and 2). It has been shown previously (e.g., [15,16]) that the acoustic wavelength Λ^{90A} does not depend on the refractive index of the sample and therefore gives the relationship $\Lambda^{90A} = \lambda_0/\sqrt{2}$. In a macroscopically isotropic sample the use of both scattering geometries yields the optoacoustic dispersion coefficient D [17,18]. In the acoustic dispersion-free case, $D = f^{180}/(f^{90A}\sqrt{2})$ gives the refractive index n [17] at the laser wavelength λ_0 (f^{90} and f^{180} are the phonon frequencies measured in the 90A- and 180-scattering geometry, respectively).

Figures 1 and 2 show representative spectra of four samples annealed as described below (see Table I). Figure 1 gives the 90A spectrum of the fully amorphous (as-sputtered) sample supported on a glass slide; this is in contrast to samples (1)–(6), which were sputtered onto silicon. Because of the low thickness of the sample film, the spectrum shows both the longitudinally polarized phonon frequency of the sample (L) and the longitudinal phonon lines of the glass substrate (G). The intensity relation between the phonon lines of the glass substrate and the sample is about 30 and reflects the recent experimental improvements in the field of BS investigations on thin films [19]. In order to simplify the deconvolution of the longitudinal phonon lines we have prevented the appearance of the transverse signals using VV scattering (vertical polarization of the incident laser light and vertical polarization of the scattered light) [20]. The resulting sound velocity of the sample amounts to $v = 3538$ m/s and is rather low in comparison to the glass but is close to

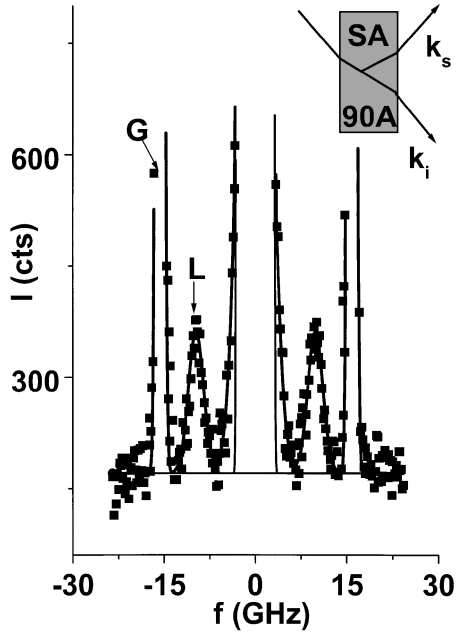

FIG. 1. Brillouin spectrum of PTC measured with the 90A-scattering geometry and the related nonlinear least square fits of an amorphous sample deposited on glass. SA: sample, 90A: scattering geometry defined by the sample habit and the light vectors k_i and k_s, f: phonon frequency in GHz, I: intensity in counts, G: longitudinal phonon line of the glass substrate, L: longitudinal phonon line of the homogeneous sample.

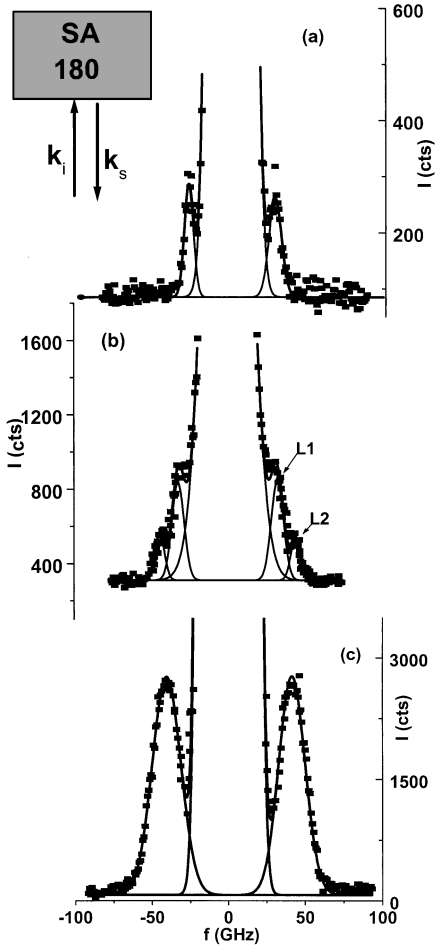

FIG. 2. Representative Brillouin spectra of PTC measured in the 180-scattering geometry and related nonlinear least square fits. (a) Sample (3), $T_a = 773$ K; (b) sample (4), $T_a = 823$ K; (c) sample (6), coarse grained state. 180: scattering geometry defined by the sample habit and the light vectors k_i and k_s, f: phonon frequency in GHz, I: intensity in counts, L1, L2: longitudinal phonon lines of the phase-separated sample.

that of glassy polymers [17]. Using 180 scattering these measurements have been repeated on the as-sputtered sample (1). Both results enabled us to calculate an optoacoustic dispersion coefficient $D \approx n = 2.4$. Within the margin of error this value coincides with that obtained by ellipsometry, suggesting the absence of any hypersonic relaxation processes. Figures 2(a)–2(c) show the Brillouin spectra of samples (3) and (4) and of the coarse grained sample (6). Sample (3) was annealed at $T_a \approx 773$ K just below the critical annealing temperature $T_{ca} \approx 823$ K, and sample (4) was annealed at T_{ca}. Applying white light at grazing incidence, sample (4) looked slightly hazy. Its spectrum [Fig. 2(b)] reflects the coexistence of longitudinally polarized phonon frequencies confirming a macroscopic phase separation within the scattering volume ($\approx 50 \times 50 \times 1.2\ \mu m^3$) already indicated by the haziness of the sample. In order to obtain the two well defined phonon lines of Fig. 2(b), the scattering volume must consist of two kinds of elastically very different grains with diameters beyond the acoustic wavelength.

Figure 3 shows the elastic stiffness moduli c_{11} as well as the hypersonic attenuation Γ_{11} of PTC as a function of the annealing temperature T_a. It is obvious that $c_{11}(T_a)$ undergoes a significant softening up to $T_a \approx 800$ K [(1)–(3)]; the figure then shows a phase coexistence at 823 K (4); for $T \geq T_{ca} = 823$ K the stiffness increases discontinuously to that of the coarse grained state (6); and the difference between the lowest and the highest stiffness modulus amounts to a remarkable 67%. It is interesting to note that the elastic stiffness of the nanostructured state [(4, upper data point) and (5)] is larger than the stiffness of the coarse grained one (6). This would be consistent with clusters of nanosized cubic crystallites of PTC having a larger orientation-averaged longitudinal modulus than the related tetragonal structured crystals of the coarse grained state.

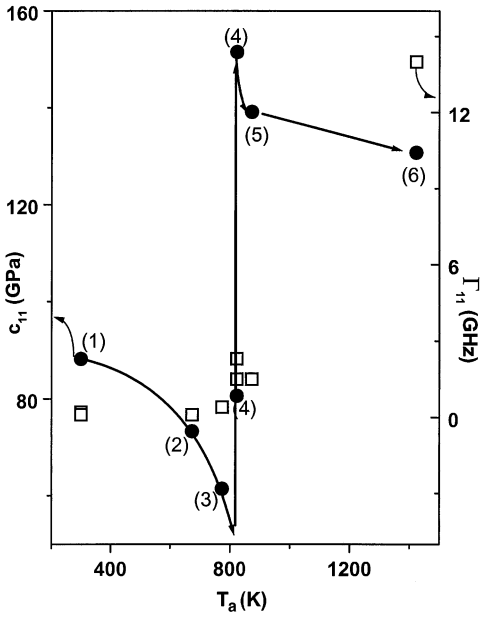

FIG. 3. Elastic stiffness moduli c_{11} and hypersonic attenuation Γ_{11} of differently annealed PTC. T_a is the annealing temperature. The straight lines in this figure only represent a guide for the eye.

As a further unexpected result, the phenomenon of the softening of $c_{11}(T_a)$ on approaching the nanosized state implies that this softening takes place within the amorphous state instead of the nsS. In order to make the calculation of $c_{11}(T_a)$ we used the average density 7050 kg/m^3 given above. A reduction in the density of the material towards the nanocrystalline state would yield a further decrease of the stiffness around T_{ca} and thus amplify the softening behavior of $c_{11}(T_a < T_{ca})$. According to Table I samples (1)–(3) are still amorphous with an average grain size of 1 nm. Tentatively, we relate the slowing down of $c_{11}(T_a < T_{ca})$ to frozen precursors of the nsS within the amorphous state. The elastic slowing down is stopped at $T_{ca} \approx 823$ K where the sputtered and subsequently annealed PTC probably realizes nanocrystalline clusters of sufficient size (in order to produce its own phonon line L2) embedded in a subnanocrystalline matrix. It should be stressed that the coexistence of isolated nanosized particles in an amorphous matrix would be incompatible with the observation of two longitudinally polarized phonons at T_{ca}. Recently, Mon [13] has predicted for nanofibers a significant sound velocity reduction only for rod diameters below 4 nm. In accordance with these predictions the position of the phonon line L1 in Fig. 2 is consistent with any stiffness reduction predicted for the subnanocrystalline state. Thus, $c_{11}(T_{ca})$ there yields a stiffness much smaller than that of the microcrystalline state (6) and still smaller than the stiffness of the pure amorphous state (1).

Defect relaxations have been discussed as a possible source for the stiffness suppression in nsM [10]. Therefore, we also have analyzed the influence of the annealing on the hypersonic attenuation. According to Fig. 3 the temporal attenuation coefficient $\Gamma_{11}(T_a)$ is, in the margin of the resolution of our tandem spectrometer, almost zero; a slight increase of $\Gamma_{11}(T_a)$ appears at T_{ca}. This result is in agreement with the observation that the optoacoustic dispersion coefficient D yields the refractive index. The strongly increased Γ_{11} of sample (6) is provoked by acoustic scattering and the appearance of acoustic anisotropy in the coarse grained state, reinforced by the strongly increased scattering volume of this bulk sample. As a matter of fact, the slowing down of c_{11} is not related to a hypersonic attenuation anomaly. Internal friction therefore can be excluded as a cause for the elastic softening.

Based on free-energy simulations, Wang *et al.* [6] have postulated the existence of a phase transformation between the nsS and the frozen amorphous state, both states being nonergodic. It is worth noting that such a structural transformation would affect both the shear and the longitudinal stiffness. Unfortunately, these authors do not discuss the effect of a structural transformation from the nsS to the amorphous state on the elastic stability of the

system. However, it seems to us that the shear instability observed by Rehn *et al.* [1] in the course of forced solid-state amorphization of Zr_3Al as well as our results on thermally induced crystallization of amorphous PTC can be taken as direct evidences for the phase transformation predicted by Wang *et al.*

This work was kindly supported by the Sonderforschungsbereich 277. We thank K. Knorr and C. Brierley for fruitful discussions.

[1] L. E. Rehn, P. R. Okamoto, R. Bhadra, and M. Grimsditch, Phys. Rev. Lett. **59**, 2987 (1987).
[2] H. Gleiter, Prog. Mater. Sci. **33**, 223 (1989).
[3] H. Gleiter, Nanostruct. Mater. **1**, 1 (1992).
[4] M. B. Bush, Mater. Sci. Eng. **A161**, 127 (1993).
[5] H. Gleiter, Nanostruct. Mater. **6**, 3 (1995).
[6] J. Wang, D. Wolf, S. R. Phillpot, and H. Gleiter, Philos. Mag. A **73**, 517 (1996).
[7] D. Korn, A. Morsch, R. Birringer, W. Arnold, and H. Gleiter, J. Phys. (Paris), Colloq. **49**, C5-769 (1988).
[8] M. Weller, J. Diehl, and H.-E. Schaefer, Philos. Mag. A **63**, 527 (1991).
[9] N. P. Kobelev, Ya. M. Soifer, R. A. Andrievski, and B. Gunther, Nanostruct. Mater. **2**, 537 (1993).
[10] N. A. Akhmadeev, N. P. Kobelev, R. R. Mulyukov, Ya. M. Soifer, and R. Z. Valiev, Acta Metall. Mater. **41**, 1041 (1993).
[11] Ya. M. Soifer and N. P. Kobelev, Nanostruct. Mater. **6**, 647 (1995).
[12] H. Kung, T. R. Jervis, J.-P. Hirvonen, J. D. Embury, T. E. Mitchell, and M. Nastasi, Philos. Mag. A **71**, 759 (1995).
[13] K. K. Mon, J. Appl. Phys. **80**, 2739 (1996).
[14] B. Jimenez, J. Mendiola, C. Alemany, L. del Olmo, L. Pardo, E. Maurer, M. L. Calzada, J. de Frutos, A. M. Gonzalez, and M. C. Fandiño, Ferroelectrics **87**, 97 (1988).
[15] E. Sawaguchi, T. Mitsuma, and Z. Ishii, J. Phys. Soc. Jpn. **11**, 1298 (1956).
[16] H. Schmitt, C. Ziebert, J. K. Krüger, C. Bruch, P. Huber, T. Knoblauch, and B. Jimenez (to be published).
[17] J. K. Krüger, in *Optical Techniques to Characterize Polymer Systems*, edited by H. Bässler (Elsevier, Amsterdam, 1989), p. 429.
[18] J. K. Krüger, R. Jimenez, K.-P. Bohn, J. Petersson, J. Albers, A. Klöpperpieper, E. Sauerland, and H. E. Müser, Phys. Rev. B **42**, 8537–8547 (1990).
[19] J. K. Krüger, Phys. Rev. B (to be published).
[20] R. Vacher and L. Boyer, Phys. Rev. B **6**, 639 (1972).